Cellular transduction of mechanical oscillations in plants by the plasma-membrane mechanosensitive channel MSL10

Daniel Tran, Marjorie Guichard, Sébastien Thomine, Nathalie Leblanc-Fournier, Bruno Moulia, Emmanuel de Langre, Jean-Marc Allain, Jean-Marie Frachisse

Cellular transduction of mechanical oscillations in plants by the plasma-membrane mechanosensitive channel MSL10

Daniel Tran[1], Tiffanie Girault[1], Marjorie Guichard[1], Sébastien Thomine[1], Nathalie Leblanc-Fournier[2,3], Bruno Moulia[2, 3], Emmanuel de Langre[4], Jean-Marc Allain[5,6], Jean-Marie Frachisse[1]

[1] Université Paris-Saclay, CEA, CNRS, Institute for Integrative Biology of the Cell (I2BC), 91198, Gif-sur-Yvette, France.

[2] INRA, UMR 547 PIAF, F-63100 Clermont-Ferrand, France

[3] Université Clermont Auvergne, UMR 547 PIAF, F-63100 Clermont-Ferrand, France

[4] LadHyX, Ecole Polytechnique, Palaiseau, 91128 Cedex, France

[5] LMS, Ecole Polytechnique, CNRS, Palaiseau, France

[6] Inria, Université Paris-Saclay, Palaiseau, France

Key words: Mechanosensitive channel, mechanotransduction, oscillation, frequency, wind

* Corresponding author : Jean-Marie Frachisse

Email : jean-marie.frachisse@i2bc.paris-saclay.fr

ORCID iD : https://orcid.org/0000-0002-9755-6536

Abstract

Plants spend most of their life oscillating around 1 to 3 Hz due to the effect of the wind. Therefore, stems and foliage experience repetitive mechanical stresses through these passive movements. However, the mechanism of the cellular perception and transduction of such recurring mechanical signals remains an open question. Multimeric protein complexes forming mechanosensitive (MS) channels embedded in the membrane provide an efficient system to rapidly convert mechanical tension into an electrical signal. So far, studies have mostly focused on non-oscillatory stretching of these channels. Here, we show that the plasma membrane mechanosensitive channel MscS-LIKE 10 (MSL10) from the model plant Arabidopsis thaliana responds to pulsed membrane stretching with rapid activation and relaxation kinetics in the range of one second. Under sinusoidal membrane stretching MSL10 presents a greater activity than under static stimulation. We observed this amplification mostly in the range of 0.3 to 3 Hz. Above these frequencies the channel activity is very close to that under static conditions. With a localization in aerial organs naturally submitted to wind-driven oscillations, our results suggest that the mechanosensitive channel MSL10, and by extension MS channels sharing similar properties, represents a molecular component allowing the perception of oscillatory mechanical stimulations by plants.

Significance Statement

Mechanosensitive (MS) channels embedded in the membrane provide an efficient system to rapidly convert mechanical tension into a biological signal. Here we show that the plasma membrane mechanosensitive channel MSL10 responds to pulsed membrane stretching with rapid activation and relaxation kinetics allowing fast adjustment of its activity to fluctuations in membrane tension. Under sinusoidal membrane mechanical stimulation, we found that MSL10 amplifies oscillatory signals near 1 Hz which corresponds to the frequencies of plant

motions in the wind. Together with its localization in aerial organs, our results indicate that the mechanosensitive channel MSL10 represents a molecular component for the perception of oscillations triggered by the wind in plants.

Introduction

Throughout their life, plants are submitted to recurrent cyclic mechanical loading due to wind. The resulting passive oscillation movements of stems and foliage is an important phenomenon for biological and ecological processes such as photosynthesis [1–3] and thermal exchange [4]. The motions induced are well described and analyzed at the whole plant scale, with oscillations at typically 1 to 3 Hz in trees [5–10]. In animals, transduction of vibrational stimulation is achieved through MS channels in organs with specialized structures, such as the ear in which the different frequencies are spatially separated[11], or as in touch perception accomplished through organ motion [12]. In plants, such specialized features have not yet been reported, and it remains unclear whether and how MS channels participate in the perception of oscillatory stimuli. To investigate this question, we studied MSL family members, homologues of the Mechanosensitive channel of Small conductance (MscS) from *E. coli* [13–15], as they are found in all land plant genomes [16]. We have focused our study on the plasma membrane-localized MSL10 [17,18].

Results and Discussion

Oscillatory movement of the stem and expression pattern of *MSL10*.

To characterize the response of Arabidopsis to wind mechanical stimulation, we examined the frequency of free oscillations of plants with a young flowering stem subjected to a short air pulse (SI Appendix, Movie 1). Using the Vibration Phenotyping System[19] (https://vimeo.com/213665517) we determined the image correlation coefficient depicting the

pendulum movement of the stem on 6 plants and obtained a mean frequency of 2.8±1.0 Hz (mean ±SD, n=131) (Fig. 1a). This frequency is among those excited by the wind[20]. Then, to determine whether MSL10 localization is compatible with a function as oscillation sensor, we characterized its expression pattern in plants at the flowering stage. Signal from a GUS reporter driven by the *MSL10* promoter was present in stem and leaf vasculature and at the root tip (Fig. 1b, c) [17]. This expression pattern of *MSL10*, especially at the junction between roots and shoots, which experiences the major tension induced by leaves and stem motion, is an expected location for probing the motion induced by the wind (Fig. 1d).

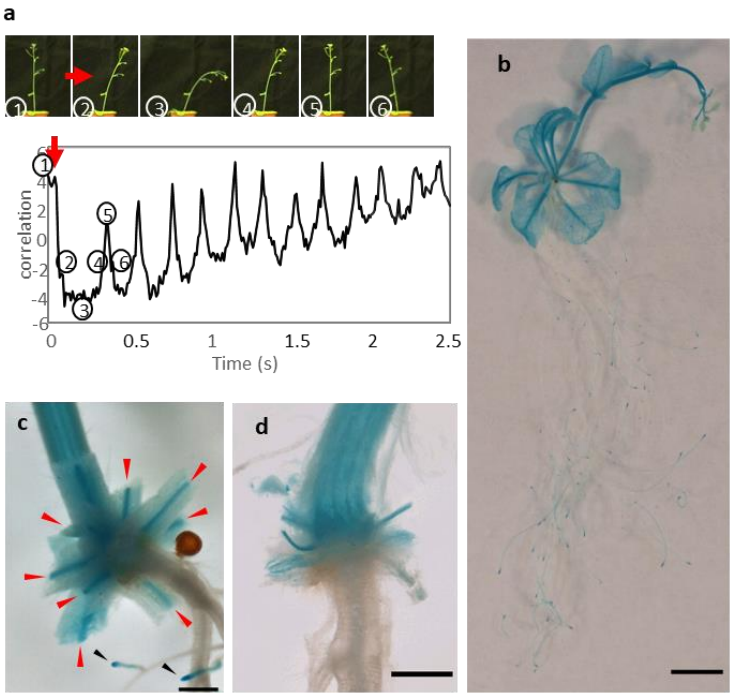

Figure 1 | Oscillatory movement and *MSL10* expression pattern in aerial part of Arabidopsis plants.

a, Top, Images of the oscillatory movement of the stem induced by an air pulse of 60 ms. **Bottom**, the correlation coefficient curve visualizes the oscillating and the damping of the stem movement (red arrow: air pulse), **b-d** Blue staining represents the β-glucuronidase (GUS) activity driven by the promoter of *MSL10*. **b,** in the root tip (indicated by black arrows in c) and throughout vasculature of the leaves and stem, **c**, at the bottom of leaf petioles (red arrows) and **d,** in the root-stem junction (d is the same view as c, with petioles entirely removed). Scale: b, 5mm; c and d, 500µm.

Kinetics characterization of MSL10 in response to pressure steps.

Channel kinetic properties are crucial for its ability to perceive oscillatory stimulation at various frequencies. In order to know how quickly MSL10 responds to variations in

membrane mechanical tension, we characterized the kinetics of this channel using the patch-clamp technique combined with a "High Speed Pressure Clamp" system[21]. To specifically monitor MSL10 activity in its endogenous environment, we expressed the *MSL10* gene in protoplasts from a quintuple mutant (*Δ5*) lacking the activity of five *MSL*-encoding genes (*msl4;msl5;msl6;msl9;msl10)*. This provides a low background to record mechanically-activated currents from *MSL10*-expressing protoplasts (*Δ5+MSL10*) [17] by applying pulses of pressure whilst monitoring transmembrane currents at a constant voltage (-186mV) on an excised membrane patch in the outside-out configuration (Fig. 2a). At this physiologically relevant membrane potential, opening of a single stretch-activated channel caused a current variation of 19.4 ± 1.7 pA (Fig. 2a, n=14) as reported in root protoplasts expressing MSL10[17,22]. We previously provided evidence that, similar to MscS of E. coli, MSL10 activates in response to lateral membrane tension increase [17]. Our finding of a linear relationship of the pressure for half-activation of the channel ($P_{0.5}$) with the pipette resistance indicates that a larger patch of membrane is activated before a small patch. This behavior as well is in favor of a regulation of MSL10 channel by membrane tension induced by pressure (SI Appendix, Fig. 2d). The sustained activity of MSL10 under membrane tension without inactivation clearly distinguishes it from its E. coli MscS homolog [23] and from the rapidly activated calcium MS channel (RMA) co-residing in the same membrane [24,25]. We observed that the activation of MSL10 current increased exponentially in response to pressure, with time constants τ_{act} ranging from 1000 ms at 30 mmHg to 200 ms at 100 mmHg (Fig. 2b and SI Appendix, Fig. 1, n = 15). The values of the activation time constants should be used with caution as activation of the channels with pressure increase depends on the patch geometry (see SI Appendix, Fig. 2b). Another bias may come from the variable number of channels in the patch: the more channels, the more visible the activation at any pressure The mean current pressure relationship was obtained by averaging individual curves with different $P_{0.5}$ (see SI Appendix, Fig. 2b), which leads to a smoothening

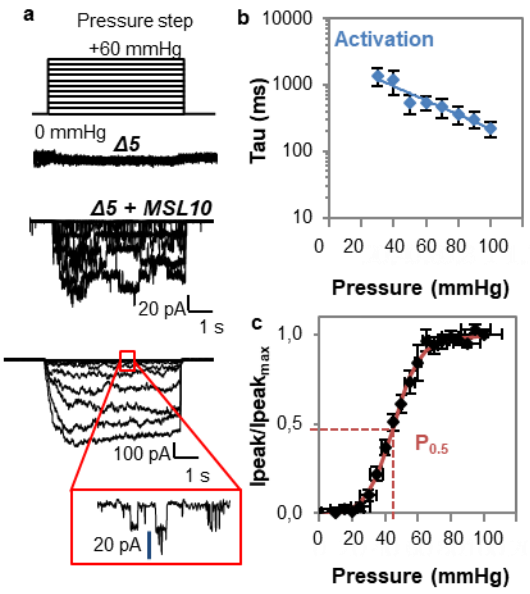

Figure 2 | Gating kinetics and pressure dependence of MSL10 in native membrane.

a, Quintuple mutant (*Δ5*) stimulated by increasing pressure steps in outside-out patch configuration shows no mechanically activated current. *Δ5* mutant expressing MSL10 (*Δ5+MSL10*) shows currents stimulated in outside-out configuration by increasing pressure steps with slow activation kinetics. We assume that variation in current amplitude among patches is due to variation in channel density due to the expression of the protein. With chloride as main charge carrier (158 mM cytosolic side/110 mM external side), single channel amplitude shows current transitions of 19.4 ± 1.7 pA at -186 mV (n = 14 protoplasts). **b,** Pressure dependence of activation time constant for MSL10 in the excised outside-out-patch configuration (SI Appendix, Fig. 1). Results are normalized to the $P_{0.5}$ of each patch and data represent mean ± S.E.M (n = 15 protoplasts). **c,** I_{max} normalized current–pressure relationship of stretch-activated currents (SI Appendix, Fig. 2) in excised outside-out-patch configuration in *Δ5+MSL10*, fitted with a Boltzmann equation. $P_{0.5}$ of 49.3 ± 3.4 mmHg is the average value determined for individual cells. Data represent mean ± S.E.M (n = 15 protoplasts).
The membrane potential is clamped at -186 mV. MSL10 protein is transiently expressed in quintuple *msl4;msl5;msl6;msl9;msl10* mutant (*Δ5*) protoplasts. Ionic conditions are described in the Materials and Methods.

of the variation of the opening probability with pressure. The mean current-pressure relationship representing the MSL10 channel sensitivity to membrane tension was well described by a Boltzmann function with a pressure for half-activation ($P_{0.5}$) of 49.3 ± 3.4 mmHg, an activation threshold of about 30 mmHg and a saturation pressure of about 70 mmHg (Fig.2c and SI Appendix, Fig. 2a-c).

MSL10 enables the perception of oscillatory stimulations.

We then examined the effect of oscillatory membrane tension on MSL10 channel activity. In order to set the pressure protocol we first submitted the membrane excised patch to various frequencies. As illustrated in Figure 3, shifting from a static pressure (0 Hz) to a

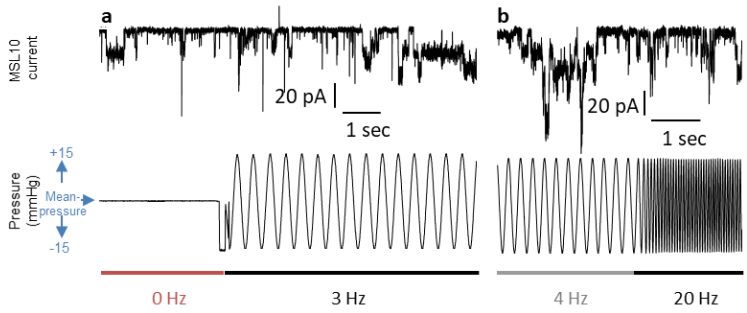

Figure 3 | MSL 10 channel activity is dependent on the frequency of the pressure stimulation.

a, Channel activity is greater upon oscillatory pressure stimulation compared to static pressure stimulation. Representative recording of single channel activity of MSL10 in response to static pressure followed by an oscillatory pressure stimulation of 3 Hz at +15/-15 mmHg, **b**, channel activity decrease when increasing the excitation frequency from 4 Hz to 20 Hz.

MSL 10 activity is recorded in the excised outside-out-patch configuration, in response to static (0 Hz) or oscillatory pressure stimulation of +15/-15 mmHg at 3 Hz, 4 Hz and 20 H. The membrane potential is clamped at -186 mV. MSL10 protein is transiently expressed in (Δ5) protoplasts. Ionic conditions are described in the Materials and Methods

sinusoidal pressure of 3 Hz induced channel activation, while increasing the frequency of the oscillatory pressure from 4 Hz to 20 Hz decreased the channel activity. To determine whether channel activity was modulated by frequency, MSL10 activity was recorded under oscillating pressures at a wide range of frequencies from 0.3 to 30 Hz (Fig. 4a and SI Appendix, Movie 2). Whatever the frequency tested, opening events occurred almost exclusively during the upper phase of the period (≥ 80 % of cases) (Fig. 4b, SI Appendix, Fig. 3). At low frequency (≤ 1 Hz), at least one opening transition of the channel was triggered during each period, (Fig. 4c, 100 % of cases), at 3 Hz 70 % of the periods triggered channel opening, while at 30 Hz only 20 % of the periods were effective (Fig 4c and SI Appendix, Fig. 4). Thus, the channel does not open randomly in response to oscillatory stimulations (SI Appendix, Fig. 3, SI Appendix, Movie 2).

We then undertook a comparison between static and oscillatory stimuli using a protocol alternating the two types of stimulations (see Fig. 4d). A static stimulation held at a "mean-pressure" slightly lower than $P_{0.5}$ (mean pressure is the average of the sinusoidal pressure) was

applied for 1 min followed by a sinusoidal pressure stimulation of +/-15 mmHg from the mean-pressure baseline at a given frequency for 1 min. This protocol was repeated to sweep frequencies from 0.3 to 30 Hz and then from 30 to 0.3 Hz, always with the same mean-pressure, in order to determine the effect of frequencies on channel activity compared to static stimulation (Fig. 4d). Figure 4e-g shows the relative effect of frequencies (ratios oscillatory/static) on NP(o), τ_{open} and τ_{close} on at least 5 membrane patches. NP(o) is the probability that a channel is

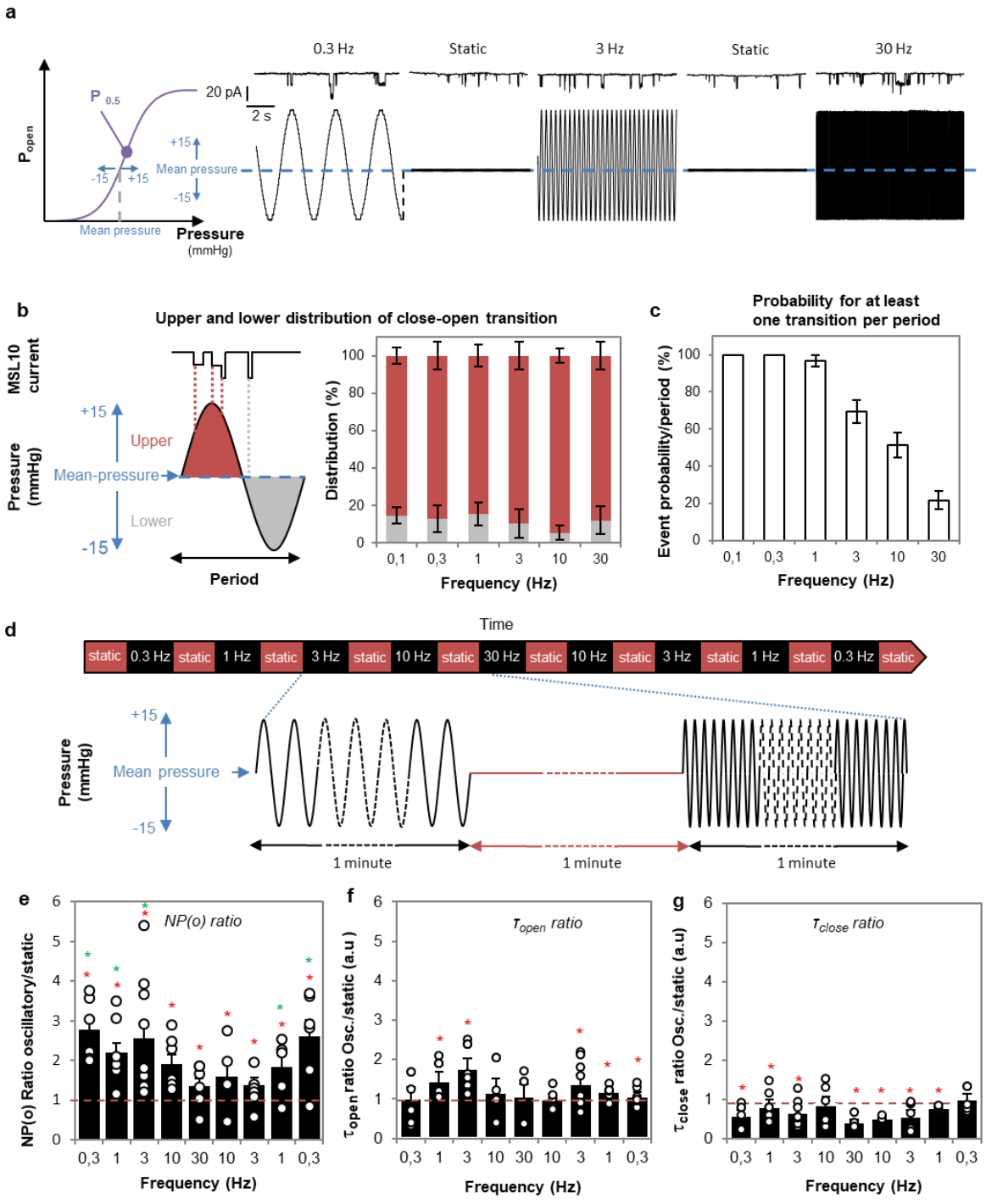

Figure 4 | Effect of oscillatory pressure stimulation on MSL10 channel activity.
a, Representative recording of single channel activity of MSL10 in the excised outside-out-patch configuration, in response to stimulations alternating static and oscillatory pressure at 0.3 Hz, 3 Hz and 30 Hz. An oscillatory pressure of +15/-15 mmHg from a mean pressure is applied. **b,** *Left*, Idealized MSL10 current used for event analysis in response to oscillatory pressure. *Right*, Distribution of close-open transitions (at least one) elicited at upper (red bars) or lower (light grey bars) pressure as a function of frequency for 15 seconds of loading. Results represent mean ± S.E.M (n ≥ 5 protoplasts). **c,** Probability that the MSL10 channel undergoes at least one close-open transition per period as a function of frequency. Results represent mean ± S.E.M (n ≥ 5 protoplasts). **d,** Sequences of 1 min oscillatory pressure alternating with 1 min static pressure are performed on excised outside-out-patches over time. The oscillatory stimulation (same protocol for SI Appendix, Fig. 5a-c) is of 30 mmHg amplitude (+15/-15 mmHg from a mean-pressure level) with a sweep of frequencies from 0.3 to 30 Hz (**--**), while static stimulation is at mean-pressure (--). **e-g,** Relative effect of frequency (oscillatory/static mean-pressure) on **e,** open probability NP(o), **f,** open state time constant and **g,** closed state time constant. The red dashed line represents the relative ratio static/static (=1). Each point represents each biological replicate (n ≥ 5 for a given frequency); asterisk in red (*) indicates in **e**, **f** and **g** that mean value is significantly different from 1 (Mann-Whitney Rank Sum Test, p<0.05), asterisk in green (*) in **e** indicates mean NP(o) is significantly different from mean NP(o) obtained at 30 Hz (Mann-Whitney Rank Sum Test, p<0.05).
MSL 10 activity is recorded in the excised outside-out-patch configuration. The membrane potential is clamped at -186 mV. MSL10 protein is transiently expressed in (Δ5) protoplasts. Ionic conditions are described in the Materials and Methods

open (multiplied by the number of channels present in the patch: it is thus the mean of the current integrated over a period and normalized by the current of a single channel (19.4pA). τ_{open} and τ_{close} are the characteristic time constants that a single channel spends in the open and close state, respectively: they are obtained from the single channel events as visible on figure 4a. Under static pressure, they can be related to the invert of k_{off} and k_{on}, respectively.

A ratio (NP(o) osc/ NP(o) stat) above 1 indicates a higher activity of the channel under sinusoidal stimulation than under static stimulation. We observed that at each frequency, the NP(o) ratio is significantly greater than one, meaning that the mean open probability is significantly higher upon dynamic than static stimulation, while the pressure applied was on average the same (Fig. 4e; red asterisks, Mann-Whitney Rank Sum Test, $p \leq 0.05$). The highest ratios are observed at low frequency (0.3, 1 and 3 Hz), which correspond to the frequencies of plant oscillation measured in Figure 1a (Fig. 4e, green asterisks, Mann-Whitney Rank Sum Test, $p \leq 0.05$). The asymmetry observed in NP(o) distribution for decreasing and increasing frequencies (Fig. 4e and SI Appendix, Fig.5a) likely reflect the diminution of the number of active channels over the experiment. Since we were not able to recover activity, even after 15 min without applying any pressure, we attributed this decrease in the number of active channels to a rundown. SI Appendix, Figure 5 illustrates the effect of frequencies on NP(o), τ_{open} and τ_{close} obtained for a representative recording. Under oscillatory stimulation, NP(o) increased, τ_{open} did not change, while τ_{close} decreased compared to the static stimulation. In order to further

quantify the opening and closing oscillation dependency of MSL10, we compared open and close time constants obtained from five patches, either under static or dynamic conditions. We measured a mean open time constant under static condition of τ_{open} static = 14.7 ± 1.9 ms (n ≥ 5). This time constant is not appreciably affected by oscillatory stimulation with a τ_{open} oscillation relative to static above 1 (Fig. 4f). The mean close time constant τ_{close} decreased significantly from τ_{close} static = 164.5 ± 24.8 ms to τ_{close} oscillation = 106.4 ± 17.6 ms (all frequencies, n ≥ 5). The ratios τ_{close} osc/τ_{close} stat were lower than 1 (Fig. 4g), suggesting that MSL10 spends less time in the closed state due to an increase in their opening probability upon oscillatory stimuli.

MSL10 channel behaves as a double state oscillatory transduction system.

Mammalian Piezo1 and Piezo2 have been reported to behave as pronounced frequency filters[12], thus allowing transduction of repetitive mechanical stimuli at a given frequency. This was attributed to their strong inactivation. With MSL10, contrary to what has been observed in the bacterial MscS[26,27], we did not observe a strong inactivation, but still we observed a clear oscillation dependence of channel activity in a wide range of frequencies. We tested, using a simple model, if this may come from the natural kinetic of opening and closing as a function of the tension. To do so, we implemented a two-state model not based on parameters obtained in static conditions (Fig. 2) but instead on parameters obtained in oscillatory conditions (Fig. 4; see Material & Methods). By simulating oscillatory stimulation, we were able to fit the model to the experimental data obtained upon oscillatory stimulation of MSL10 (Fig. 5). We derived kinetic parameters in the typical range of MSL10 activation ($\overline{K_o} = 2.0s^{-1}, \overline{K_c} = 14s^{-1}, P_o = 7.1\ mmHg\ and\ P_c = 9.0mmHg$, with $\overline{K_o}$ (resp. $\overline{K_c}$) the opening (resp. closing) rate at the pressure P_{mean}, and P_o and P_c the characteristic pressure on which the kinetic constants are

varying, Fig. 5a) and compatible with the parameters obtained in static conditions (Fig. 2). The 2-state model thus fits our data (Fig. 4) despite its lack of explicit frequency dependency (Fig. 5a), and is sufficient to explain the oscillatory dependence of the response.

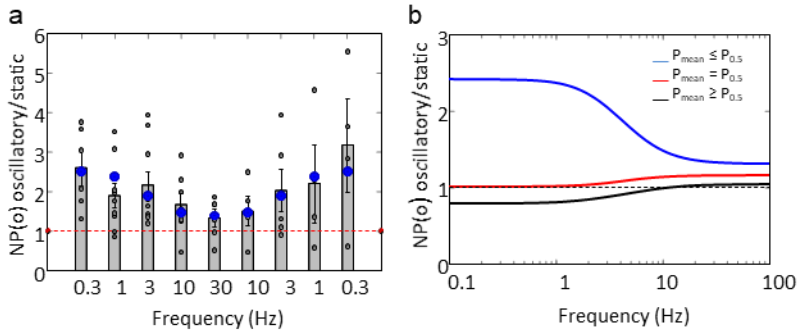

Figure 5 | Modelling of MSL 10 channel as a classical double state system.
The channel is modelled as a 2 state (open-close) system, with rates classically changing exponentially with applied pressure. No specific frequency dependence is introduced. **(a)** Adjustment of the model to experimental data. Model predictions (blue circles) are superimposed over data from Fig. 3e. **(b)** Prediction of the NP(o) ratio between oscillatory/static mean-pressure for different initial mean-pressure, using the same parameters. Blue: parameters obtained from the experiment (mean-pressure 7.6mmHg below $P_{0.5}$). Red: mean-pressure taken as $P_{0.5}$. Black: mean-pressure increased by 7.6mmHg with respect to $P_{0.5}$.

The low frequency amplification of the channel can be explained by the non-linear response of the channel to static pressures. At frequencies significantly lower than the activation rates (invert of the activation times) of the channel, the probability of channel opening is well described by its stationary value, which follows the curve of open probability versus pressure (Fig. 2c). As the mean-pressure is below $P_{0.5}$, an increase in pressure will open more channels than the same decrease in pressure. Thus, it is expected that at low frequencies the ratio is greater than one. Choosing an initial mean-pressure exactly at $P_{0.5}$ will symmetrize the effects of the increase and decrease in pressure leading to a ratio of 1 (see Fig. 5b). Starting from a pressure above $P_{0.5}$ will lead to a decrease of the ratio. The reliability of this model raises two questions: at which frequencies does the channel function and what is the mean pressure applied to the membrane *in vivo*? The free oscillations of Arabidopsis around 3 Hz that we have measured (Fig. 1a) are within the range of low frequencies in the model for which oscillatory

stimulations are more efficient than static (Fig. 5b) and are well described by the Boltzmann response. For the mean pressure applied *in vivo*, one should expect to have two contributions: a baseline due to the turgor pressure, and an additional one due to the bending during the plant oscillation, proportional to the amplitude of the plant oscillations. Thus, for a plant in resting conditions, the MSL10 channel is expected to be in the lower portion of the Boltzmann curve (Fig. 2c) wherein the channel is closed. One might speculate that for low or moderate wind, the baseline tension in the membrane lies in a domain of the Boltzmann curve below $P_{0.5}$. In these conditions, channel activity is amplified by oscillatory stimulation and efficiently transduce this signal into cellular ion fluxes. On the other hand, under strong wind, the baseline tension in the membrane would correspond to a domain of the Boltzmann curve above $P_{0.5}$. In these conditions, channel activation by sinusoidal stimulation would be lower than under static stimulation therefore damping signal transduction and preventing excessive response to high wind. This might represent a homeostatic behavior amplifying channel activity for plants under low wind but decreasing channel activity for strong wind.

At high frequency, we predict a ratio larger than 1, whatever the initial mean-pressure. This effect is due to higher pressure sensitivity for opening than for closing the channel, but is harder to explain intuitively. Interestingly, the characteristic frequency at which the channel changes from one regime to the other one does not seem to depend on the mean-pressure. This effect on the channel observed for mechanical stimulation at frequency higher than 10 Hz is difficult to rely to a cellular physiological function.

Our finding also raises the question of how oscillations occurring at the scale of the plant organ could be relayed at the scale of the cell membrane. We know that a mechanical stimulation, in order to be efficient (in term of physiological response), should produce a tissue/cell deformation[28,29]. In a previous study on Arabidopsis[30], sinusoidal sweep excitation, mimicking wind, combined with high-speed imaging allowed us to estimate several modal frequencies and

the corresponding spatial localizations of deformation. The spatial localizations of the deformation are compatible with the localizations of MSL10 expression in the plant as measured here (Fig. 1b). Therefore, to link membrane and organ scales we propose a qualitative model in which tissue/cell deformation induced by mechanical oscillations would induce local membrane tension able to trigger MSL10 channel. However, a full assessment of this hypothesis requires the modelling of the flowering stem. This approach must take into account the visco-elastic properties of the cell wall and of the plasma membrane, and the anchoring of the plasma membrane to the cell wall at specific points [31]. Then, based on the deformation all along the flowering stem during oscillatory movement, an estimation of the distribution of membrane tension variation along the shoot could be designed. Once this model of stem bending is developed it will help to link oscillations at the whole plant and the cellular scales.

Conclusion

In plants, the functions of plasma membrane-located MSLs are unknown, with the exception of MSL8 which was shown to be involved in pollen hydration[32]. Although it is involved in cell swelling response[33], functions assigned to MSL10 have not been yet specifically identified. Actually, MSL10 was shown to induce cell death, but this effect was found to be separable from its mechanosensitive ion channel activity[34,35]. In the present study we provide compelling evidence that MSL10 acts not only as a classical transducer of sustained force but also as a transducer of mechanical oscillations. In plant cells, anions accumulate in the cytoplasm [36,37]. Then the highly negative plasma membrane potential together with the anion concentration gradient drive passive fluxes of anions out of the cell through plasma membrane anion permeable channels. Given its large conductance and its selectivity in favor of anions[17,18] fluxes mediated through MSL10 will depolarize the plasma membrane making this channel a potent actor of mechano-electric signaling [38].

This study shows that MSL10 might represent a system of oscillatory perception in plants. Our findings open new avenues for studying the molecular mechanisms involved in the perception of oscillations that allows environmental adaptation.

Methods

Histology

Transgenic *Arabidopsis* lines used for histochemical studies and carrying the *pMSL10*::*GUS* promoter-reporter gene fusion were obtained previously[17]. In order to perform detection of β-glucuronidase (GUS) activity on whole plant, plants were grown on agar plate. In this culture condition, mature plants with flowering stem have a reduced height of ~4 cm and are suitable for staining. Tissue was fixed for 30 min in ice-cold 90% acetone, then incubated overnight at 37°C in 0.5 µg/mL 5-bromo-4-chloro-3-indoyl β-glucuronic acid, 100mM $NaPO_4$ (pH 7), 0.1% Triton X-100, 5 mM potassium ferrycyanide, and 10mM EDTA. Samples were then dehydrated through an ethanol series and photographed with a camera or with a Nikon AZ100 MultiZoom macroscope (objective: AZ-Plan Apo 1X NA 0.1 WD 35 mm (Nikon)).

Callus initiation and maintenance

Arabidopsis thaliana (Col-0 accession) surface-sterilized seeds were sown on "initiation medium" containing 4.3 g/L Murashige and Skoog salts (MS, Sigma-Aldrich), 2% sucrose, 10 mg/L myo-inositol, 100 µg/L nicotinic acid, 1 mg/L thiamine-HCl, 100 µg/L pyridoxine-HCl, 400 µg/L glycine, 0.23 µM kinetin, 4.5 µM 2,4-D, 1% Phytagel (pH 5.7). For callus generation, seeds were cultured on horizontal plates in a growth chamber (Sanyo MLR-350) at 21°C with a 16-h photoperiod under 120 micromol photons m-2 s^{-1}, provided by neon tubes PHILIPS Master TL-D 90 36w/965 (2/3) and OSRAM Fluora L36w/77 (1/3), for 15 days. Calli were then transferred (same growth chamber) onto "maintenance medium"

containing 4.3 g/L MS salts (Sigma-Aldrich), 2% sucrose, 10 mg/L myo-inositol, 100 µg/L nicotinic acid, 1 mg/L thiamine-HCl, 100 µg/L pyridoxine-HCl, 400 µg/L glycine, 0.46 µM kinetin, 2.25 µM 2,4-D, 1% phytagel, (pH 5.7), and sub-cultured every 15 days onto fresh "maintenance medium".

Protoplast isolation and transient transformation

Calli from *Arabidopsis* were digested for 15 min at 22 °C under hyperosmotic conditions (2 mM $CaCl_2$, 2 mM $MgCl_2$, 1 mM KCl, 10 mM MESs (pH 5.5), 0.2 % cellulysine (Calbiochem), 0.2 % cellulase RS (Onozuka RS, Yakult Honsha Co.), 0.004 % pectolyase Y23 (Kikkoman Corporation), 0.35 % Bovine Serum Albumin (Sigma) and mannitol to 600 mOsmol. For enzyme removal, the preparation was washed twice with 2 mM $CaCl_2$, 2 mM $MgCl_2$, 10 mM MES (pH 5.5), and mannitol to 600 mOsmol. For protoplast liberation, the preparation was incubated with 2 mM $CaCl_2$, 2 mM $MgCl_2$, 10 mM MES (pH 5.5), and mannitol to 280 mOsmol. Filtering the suspension (through a 80 µm nylon mesh) yielded protoplasts. For transient expression, protoplasts were co-transformed as described by Haswell et al. (2008)[17]. Silent protoplasts obtained from quintuple mutant (Δ5) Arabidopsis calli were co-transformed with 2.5 µg p35S::GFP in the p327 vector and with 10 µg p35S::MSL10 in the pAlligator2 vector. We only used fluorescent protoplasts, indicating a co-transformation event, for patch-clamp experiments. As controls for transfection, we tested patches from Δ5 cells transfected with soluble GFP alone (n= 5) and found no mechanically activated currents in the pressure range from 0 to 60 mmHg.

Electrophysiology

Patch-clamp experiments were performed at room temperature with a patch-clamp amplifier (model 200A, Axon Instruments, Foster City) and a Digidata 1322A interface (Axon Instruments). Currents were filtered at 1 kHz, digitized at 4 kHz, and analyzed with pCLAMP8.1 and Clampfit 10 software. During patch-clamp recordings, the membrane

potential was clamped at -186 mV and the pressure was applied with a High Speed Pressure-Clamp system[39] (ALA Scientific Instrument), allowing the application of precise and controlled pressure pulses or continuous sinusoidal variations in the pipette[21]. Media were designed in order to eliminate stretch-activated K^+ currents whereas the Ca^{2+} current is negligible compared to the Cl^- current. Isolated protoplasts were maintained in bathing medium: 50 mM $CaCl_2$, 5 mM $MgCl_2$, 10 mM MES-Tris, and 0,25 mM $LaCl_3$ (pH 5.6). Membrane seal with low resistance (< 1 GΩ) and with unstable current after excision were rejected. The pipettes were filled with 150 mM CsCl, 2 mM $MgCl_2$, 5 mM EGTA, 4.2 mM $CaCl_2$, and 10 mM Tris-HEPES (pH 7.2), supplemented with 5 mM MgATP. We adjusted the osmolarity with mannitol to 450 mosmol for the bath solution and 460 mosmol for the pipette solution using an osmometer (Type 15, Löser Meβtechnik). Gigaohm resistance seals between pipettes (pipette resistance, 0.8-1.5 MΩ), coated with Sylgard (General Electric) and pulled from capillaries (Kimax-51, Kimble Glass), and the protoplast membranes were obtained with gentle suction leading to the whole-cell configuration, and then excised to an outside-out configuration. The current-pressure relationship data were fitted to a Boltzmann function

$$I = Ir + Im \cdot \frac{1}{1 + e^{(P_{0.5} - P)/P_c}}$$

where Ir is the background current at zero pressure, Im is the maximum steady state current intensity, P_c is the slope of the tangent at inflexion point and $P_{0.5}$ is the pressure of half activation.

The current activation kinetics were fitted with a mono-exponential function

$$F(t) = A \cdot e^{-t/\tau} + C$$

where *A* is current-scale coefficient, τ is the time constant and *C* maximum current intensity.

Mechanosensitive channels respond to membrane tension, which itself depends on the pipette (and patch) geometry[40,41]. Thus, as the membrane geometry is slightly different from one patch to another (SI Appendix, Fig. 2a and 2d), Boltzmann functions were determined for

each patch individually, prior to oscillatory pressure stimulation application (SI Appendix, Fig. 2a). This allows delivering the oscillatory pressure in the same zone of membrane tension sensitivity. The amplitude of the oscillation was +15/-15 mmHg from a mean-pressure baseline that we choose slightly below (5 to 10 mmHg) the $P_{0.5}$ (Fig. 4a).

Statistical analysis

The data were analysed using Student's *t*-test and analysis of variance. Comparison of *NP(o)* at different frequencies (Fig.4 and SI Appendix, Fig.5) were analysed with Rank Sum test. $NP(o)_{osc}$ was determined for each oscillatory sinusoidal pressure frequency (0.3 to 30 Hz) and $NP(o)_{stat}$ for each static stimulation prior to frequency stimulation. In figure 4e we present the ratio $NP(o)_{osc}/ NP(o)_{stat}$ called *NP(o) Ratio*. The same principle is applied for T_{open} *ratio* and T_{close} *ratio* Fig. 4f and g.

Cloning and genetics

All plasmid constructs were made with Gateway technology (Life Technologies). The *MSL10* cDNA was cloned previously into pENTR/D-TOPO[17]. This pENTR construct was then used in recombination reactions with pAlligator[42] to create the MSL10 protein overexpression construct (*p35S::MSL10*). This construct was used for transient expression in protoplasts obtained from the quintuple mutant *msl4;msl5;msl6; msl9;msl10* (Δ*5 + MSL10*).

Modeling

We modeled MSL10 as a 2 states channel: an open one (O), in which the channel is activated, and a closed one (C) in which the channel is completely closed. The equilibrium between the 2 states is given by the classical chemical reaction:

$$C \underset{k_C}{\overset{k_O}{\rightleftharpoons}} O$$

with k_o and k_c the opening and closing rates, respectively. Opening (resp. closing) rate increases (resp. decreases) exponentially with the applied pressure, describing the mechano-sensitivity in the Arrhenius framework:

$$k_o(P) = K_o e^{P/P_o}, \quad \text{and} \quad k_c(P) = K_c e^{-P/P_c}$$

with P_o and P_c the characteristic pressure on which the kinematic constants are varying.

In this minimal model, the open probability $n_o(t)$ (number of open channels/number of channels) varies as:

$$\frac{dn_o(t)}{dt} + \big(k_o(P) + k_c(P)\big)n_o(t) = k_o(P)$$

Thus, the open probability versus pressure curve (figure 2c) is given by the stationary solution:

$$n_{o\,stat}(P) = \frac{1}{1+\frac{K_c}{K_o}e^{-P\left(\frac{1}{P_c}+\frac{1}{P_o}\right)}},$$

and the activation time (figure 2c) is:

$$\tau_{act} = \frac{1}{\big(k_o(P) + k_c(P)\big)}$$

This model does not contain any active oscillatory sensitivity, but the reaction rates are affected by the changes in pressure. To determine if the model can capture the frequency-dependency of the channel response (Fig. 4e), we simulated using Matlab an oscillatory pressure of magnitude ΔP for a minute:

$$\frac{dn_o(t)}{dt} + \left(\overline{K_o}exp\left(\frac{\Delta P \sin 2\pi ft}{P_o}\right) + \overline{K_c}exp\left(-\frac{\Delta P \sin 2\pi ft}{P_c}\right)\right)n_o(t) = \overline{K_o}exp\left(\frac{\Delta P \sin 2\pi ft}{P_o}\right),$$

$$\text{with } \overline{K_o} = K_o e^{P_{mean}/P_o}, \text{ and} \qquad \overline{K_c} = K_c e^{-P_{mean}/P_c}.$$

The integral of the number of open channels during one minute is then divided by the number of open channels under static pressure P_{mean} (same equation, with $\Delta P=0$). The result is directly the NP(o) ratio presented on figure 4e at the frequency f.

We then used the fminsearch function of Matlab to minimize the distance between our solution at all frequencies and our experimental results (Fig. 4e – NP(o) ratio as a function of the frequency). We obtained the following parameters:

$$\overline{K_o} = 2.0s^{-1}, \overline{K_c} = 14s^{-1}, P_o = 7.1\,mmHg \text{ and } P_c = 9.0mmHg$$

This set is the minimization of a non-linear problem, and cannot be seen as unique. We also did not perform a sensitivity analysis to determine the coupling between parameters. Indeed, due to the errors on the measurements, due to patches variability, as well as possible degradation under sustained pressure, such analysis would bring no further information.

Note that the total number of channels is not needed due to the normalization by the response at the "mean" pressure.

The set of parameters we found gives a P_{mean} 7.7mmHg below $P_{0.5}$, in agreement with our experimental protocol. The obtained $\overline{K_o}$ and $\overline{K_c}$ are of the same order than the ones estimated from the dwell time measures (see SI Appendix, Fig. 5b&c for static pressure):

$$\overline{K_o} = \frac{1}{\tau_{close}} \approx 2s, \quad \text{and } \overline{K_c} = \frac{1}{\tau_{open}} \approx 25s.$$

Then, we used the same set of parameters and the equation to simulate the NP(o) ratio at different frequencies (from 0.1 to 100Hz) for the same P_{mean}, for a $P_{mean}=P_{0.5}$ and for a P_{mean} 7.7mmHg above $P_{0.5}$ (see Fig. 5).

Accession numbers

MSL4: At1g53470 (SALK_142497, msl4-1)

MSL5: At3g14810 (SALK_127784, msl5-2)

MSL6: At1g78610 (SALK_06711, msl6-1)

MSL9: At5g19520 (SALK_114626, msl9-1)

MSL10: At5g12080 (SALK_076254, msl10-1)

Data Availability

All data needed to evaluate the conclusions in this paper are presented in the main text and *SI Appendix*. The quintuple mutant msl4-1 msl5-2 msl6-1 msl9-1 msl10-1 used in this study is available upon order at Arabidopsis Biological Resource Center (ABRC) upon the reference Germplasm: CS69760 (https://abrc.osu.edu/stocks/number/CS69760).

References

1. Roden, J. S. Modeling the light interception and carbon gain of individual fluttering aspen (Populus tremuloides Michx) leaves. *Trees* **17**, 117–126 (2003).
2. Roden, J. S. & Pearcy, R. W. Effect of leaf flutter on the light environment of poplars. *Oecologia* **93**, 201–207 (1993).
3. Roden, J. S. & Pearcy, R. W. Photosynthetic gas exchange response of poplars to steady-state and dynamic light environments. *Oecologia* **93**, 208–214 (1993).
4. Grace, J. The turbulent boundary layer over a flapping Populus leaf. *Plant Cell Environ.* **1**, 35–38 (1978).
5. Tadrist, L. *et al.* Foliage motion under wind, from leaf flutter to branch buffeting. *J. R. Soc. Interface* **15**, 20180010 (2018).
6. Jackson, T. *et al.* An architectural understanding of natural sway frequencies in trees. *J. R. Soc. Interface* **16**, 20190116 (2019).

7. Rodriguez, M., Langre, E. de & Moulia, B. A scaling law for the effects of architecture and allometry on tree vibration modes suggests a biological tuning to modal compartmentalization. *Am. J. Bot.* **95**, 1523–37 (2008).

8. Gardiner, B., Berry, P. & Moulia, B. Review: Wind impacts on plant growth, mechanics and damage. *Plant Sci.* **245**, 94–118 (2016).

9. de Langre, E. Effects of wind on plants. in *Annual Review of Fluid Mechanics* vol. 40 141–168 (Annual Reviews, 2008).

10. de Langre, E. Plant vibrations at all scales: a review. *J. Exp. Bot.* **70**, 3521–3531 (2019).

11. Pan, B. *et al.* TMC1 Forms the Pore of Mechanosensory Transduction Channels in Vertebrate Inner Ear Hair Cells. *Neuron* **99**, 736-753.e6 (2018).

12. Lewis, A. H., Cui, A. F., McDonald, M. F. & Grandl, J. Transduction of Repetitive Mechanical Stimuli by Piezo1 and Piezo2 Ion Channels. *Cell Rep.* **19**, 2572–2585 (2017).

13. Kung, C., Martinac, B. & Sukharev, S. Mechanosensitive Channels in Microbes. *Annu. Rev. Microbiol.* **64**, 313–329 (2010).

14. Cox, C. D. *et al.* Selectivity mechanism of the mechanosensitive channel MscS revealed by probing channel subconducting states. *Nat. Commun.* **4**, 2137 (2013).

15. Martinac, B. & Kloda, A. Evolutionary origins of mechanosensitive ion channels. *Prog. Biophys. Mol. Biol.* **82**, 11–24 (2003).

16. Haswell, E. S. MscS-Like Proteins in Plants. in *Current Topics in Membranes* vol. 58 329–359 (Elsevier, 2007).

17. Haswell, E. S., Peyronnet, R., Barbier-Brygoo, H., Meyerowitz, E. M. & Frachisse, J.-M. Two MscS homologs provide mechanosensitive channel activities in the Arabidopsis root. *Curr. Biol.* **18**, 730–4 (2008).

18. Maksaev, G. & Haswell, E. S. MscS-Like10 is a stretch-activated ion channel from Arabidopsis thaliana with a preference for anions. *Proc. Natl. Acad. Sci. U. S. A.* **109**, 19015–20 (2012).

19. de Langre, E. *et al.* Nondestructive and Fast Vibration Phenotyping of Plants. *Plant Phenomics* **2019**, 1–10 (2019).

20. Stull, R. B. Mean Boundary Layer Characteristics. in *An Introduction to Boundary Layer Meteorology* (ed. Stull, R. B.) 1–27 (Springer Netherlands, 1988). doi:10.1007/978-94-009-3027-8_1.

21. Peyronnet, R., Tran, D., Girault, T. & Frachisse, J.-M. Mechanosensitive channels: feeling tension in a world under pressure. *Front. Plant Sci.* **5**, 558 (2014).

22. Peyronnet, R., Haswell, E. S., Barbier-Brygoo, H. & Frachisse, J.-M. Sensors of plasma membrane tension in Arabidopsis roots. *Plant Signal. Behav.* **3**, 726–729 (2008).

23. Boer, M., Anishkin, A. & Sukharev, S. Adaptive MscS Gating in the Osmotic Permeability Response in *E. coli* : The Question of Time. *Biochemistry* **50**, 4087–4096 (2011).

24. Tran, D. *et al.* A mechanosensitive Ca2+ channel activity is dependent on the developmental regulator DEK1. *Nat. Commun.* **8**, 1009 (2017).

25. Guerringue, Y., Thomine, S. & Frachisse, J.-M. Sensing and transducing forces in plants with MSL10 and DEK1 mechanosensors. *FEBS Lett.* **592**, 1968–1979 (2018).

26. Kamaraju, K., Gottlieb, P. A., Sachs, F. & Sukharev, S. Effects of GsMTx4 on Bacterial Mechanosensitive Channels in Inside-Out Patches from Giant Spheroplasts. *Biophys. J.* **99**, 2870–2878 (2010).

27. Belyy, V., Kamaraju, K., Akitake, B., Anishkin, A. & Sukharev, S. Adaptive behavior of bacterial mechanosensitive channels is coupled to membrane mechanics. *J. Gen. Physiol.* **135**, 641–652 (2010).

28. Moulia, B., Coutand, C. & Julien, J.-L. Mechanosensitive control of plant growth: bearing the load, sensing, transducing, and responding. *Front. Plant Sci.* **6**, (2015).

29. Coutand, C., Julien, J. L., Moulia, B., Mauget, J. C. & Guitard, D. Biomechanical study of the effect of a controlled bending on tomato stem elongation: global mechanical analysis. *J. Exp. Bot.* **51**, 1813–1824 (2000).

30. Der Loughian, C. *et al.* Measuring local and global vibration modes in model plants. *Comptes Rendus Mécanique* **342**, 1–7 (2014).

31. Frachisse, J.-M., Thomine, S. & Allain, J.-M. Calcium and plasma membrane force-gated ion channels behind development. *Curr. Opin. Plant Biol.* **53**, 57–64 (2020).

32. Hamilton, E. S. *et al.* Mechanosensitive channel MSL8 regulates osmotic forces during pollen hydration and germination. *Science* **350**, 438–441 (2015).

33. Basu, D. & Haswell, E. S. The Mechanosensitive Ion Channel MSL10 Potentiates Responses to Cell Swelling in Arabidopsis Seedlings. *Curr. Biol.* **30**, 2716-2728.e6 (2020).

34. Veley, K. M. *et al. Arabidopsis* MSL10 Has a Regulated Cell Death Signaling Activity That Is Separable from Its Mechanosensitive Ion Channel Activity. *Plant Cell* **26**, 3115–3131 (2014).

35. Basu, D., Shoots, J. M. & Haswell, E. S. Interactions between the N- and C-termini of the mechanosensitive ion channel AtMSL10 are consistent with a three-step mechanism for activation. *J. Exp. Bot.* **71**, 4020–4032 (2020).

36. Barbier-Brygoo, H. *et al.* Anion channels in higher plants: functional characterization, molecular structure and physiological role. *Biochim. Biophys. Acta BBA - Biomembr.* **1465**, 199–218 (2000).

37. Barbier-Brygoo, H. *et al.* Anion channels/transporters in plants: from molecular bases to regulatory networks. *Annu. Rev. Plant Biol.* **62**, 25–51 (2011).

38. Douguet, D. & Honoré, E. Mammalian Mechanoelectrical Transduction: Structure and Function of Force-Gated Ion Channels. *Cell* **179**, 340–354 (2019).

39. Besch, S. R., Suchyna, T. & Sachs, F. High-speed pressure clamp. *Pflüg. Arch. Eur. J. Physiol.* **445**, 161–6 (2002).

40. Suchyna, T. M., Markin, V. S. & Sachs, F. Biophysics and Structure of the Patch and the Gigaseal. *Biophys. J.* **97**, 738–747 (2009).

41. Lewis, A. H. & Grandl, J. Mechanical sensitivity of Piezo1 ion channels can be tuned by cellular membrane tension. *eLife* **4**, (2015).

42. Bensmihen, S. *et al.* Analysis of an activated ABI5 allele using a new selection method for transgenic Arabidopsis seeds. *FEBS Lett.* **561**, 127–131 (2004).

Acknowledgements

This work is supported by the grant ANR-09-BLAN-0245-03 from the Agence Nationale de la Recherche (ANR, project SENZO) and the grant ANR-11-BSV7-010-02 from the Agence Nationale de la Recherche (ANR, project CAROLS). This work benefits from the support of the LabEx Saclay Plant Sciences-SPS (ANR-10-LABX-0040-SPS). We would like to thank Dr. Alexis De Angeli (I2BC, Gif-sur-Yvette, France) for his help and for insightful discussions, Dr. Elizabeth Haswell (Washington University, St. Louis, USA) for providing quintuple msl mutant and GUS reporter lines, Marianne Doehler for technical assistance in

the experiments, Christelle Espagne for technical assistance, Romain Le Bars (I2BC, Imagerie-Gif Facilities), Pascal Hémon for video recording (LadHyX, CNR-Polytechnique), Gwyneth C. Ingram for corrections on the manuscript (ENS, Lyon, France).

Author Contributions

D.T performed experiments; T.G made the cloning; D.T, M.G, N.L.F, B.M, E.dL, J.M.A and J.M.F where involved in study design; J.M.A. made the modelling; D.T, J.M.A and J.M.F analyzed data; D.T, ST, JMA and J.M.F wrote the paper. All authors discussed the results and commented on the manuscript.

Author information

The authors declare no competing financial interest. Correspondence and requests for materials should be addressed to J.M.F (jean-marie.frachisse@i2bc.paris-saclay.fr).

Supplementary Data

Figure S1 to Figure S5

Movie S1 (separate file). Oscillatory movement of an Arabidopsis thaliana plant after elicitation by an air pulse. Slow motion X 16.

Movie S2 (separate file). Activation of the mechanosensitive channel MSL10 elicited by oscillatory pressure of 0.1 Hz, 1 Hz, 3 Hz.

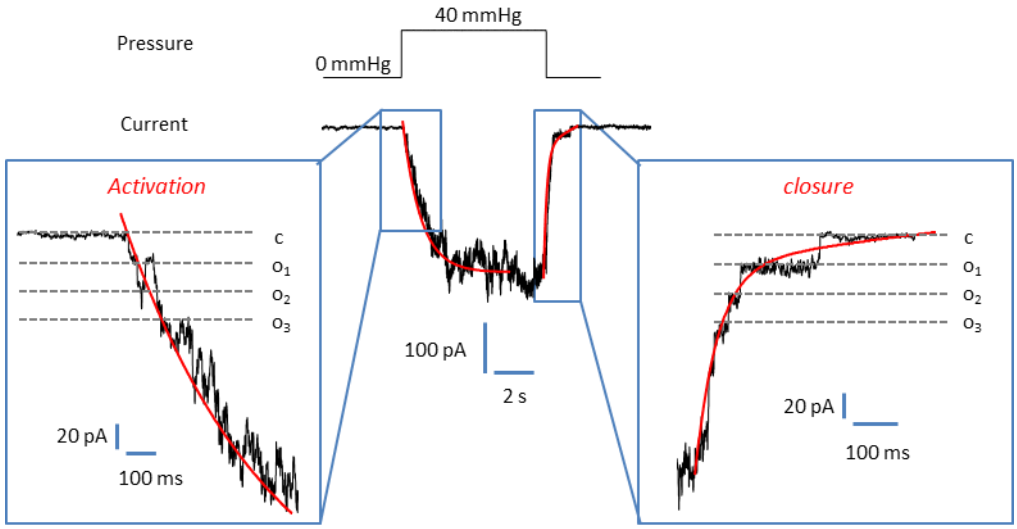

Fig. S1. MSL10 pressure dependence of activation time constant. Typical analysis of activation current from quintuple mutant expressing MSL10 elicited by pressure pulses. Current is fitted with a mono-exponential function. Insets show single current transitions happening during pressure steps. Opening (left inset: o1, o2 and o3) and closing (right inset: o3, o2 and o1) of three channels can be seen in this recording.

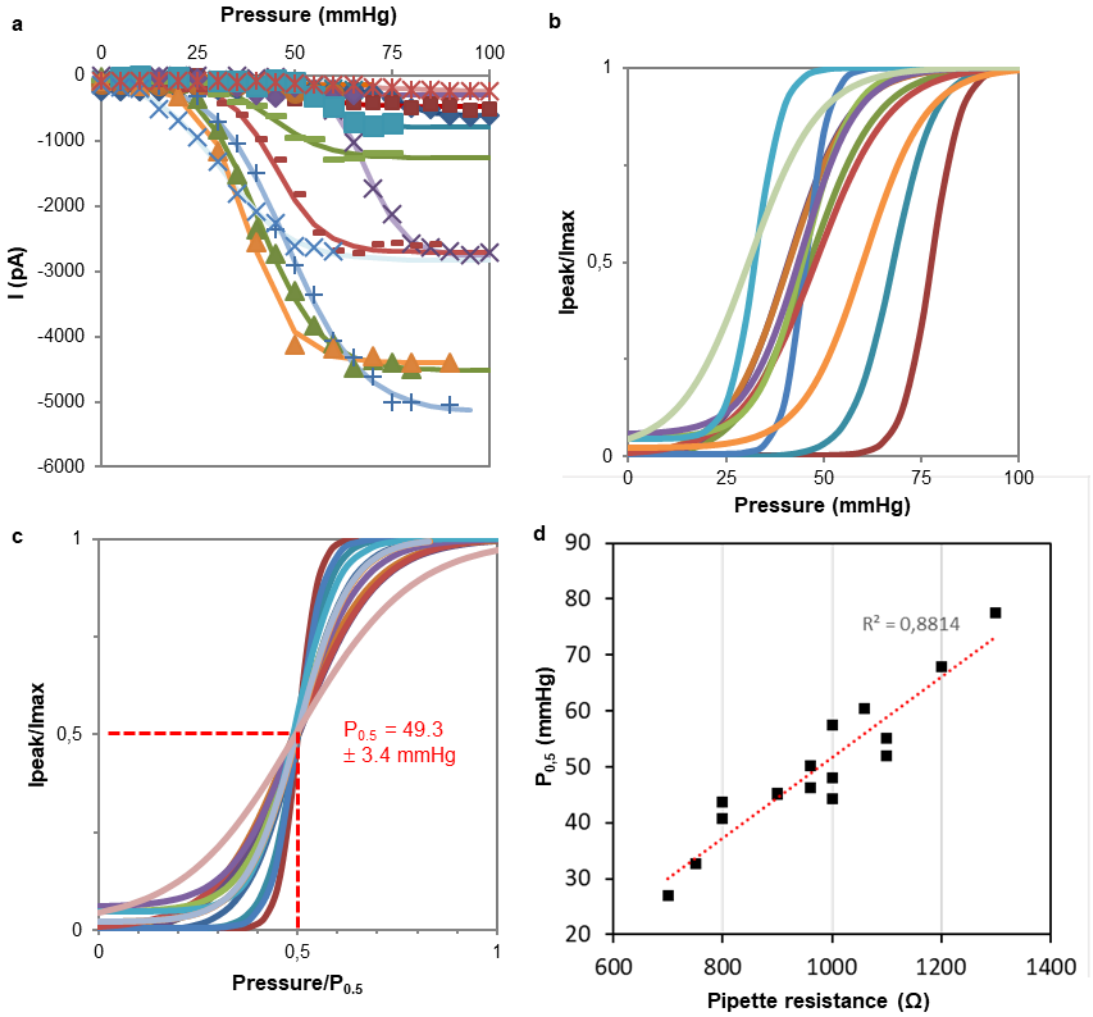

Fig. S2. Determination of current-pressure relationship of MSL10 channel. a, Current-pressure relationships recorded in different patches and fitted with a Boltzmann function. Although single activities of MSL10 channels are observed in each recording, we assume that variation in current amplitude among patches is due to the variation in channel density due to the expression of the protein. This reflects different channel densities due to heterogeneity of expression levels between protoplasts. b, In order to compare patches, we normalized each curve by maximum current amplitude (Imax) and c, the curves were then normalized to the half-maximal activation point (P0.5) from different patches. d, Relationship between the pipette resistance and the pressure of half activation (P0.5). A linear dependence of pipette resistance (geometry) with MSL10 channel activation is observed. This is in accordance with Laplace's law showing that the MSL10 channel is regulated by membrane tension, which is a general feature for MS channels[1,2,3].

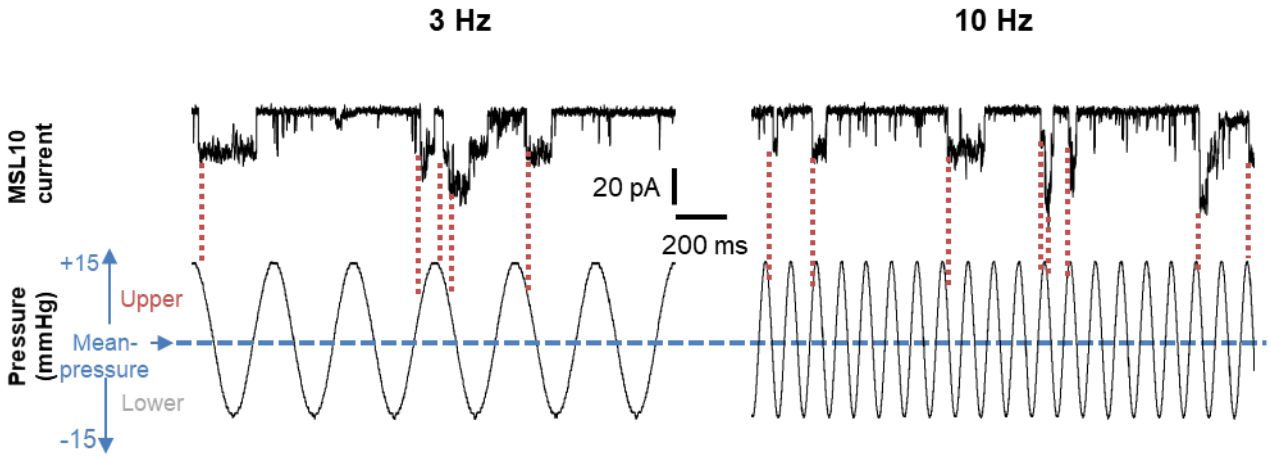

Fig. S3. MSL10 channel opening occurred almost exclusively during the upper phase of the stimulation period. Example of recording for stimulation at a frequency higher than 1 Hz (in this recording 3 and 10 Hz) we observed misfiring. Although it is the positive (not negative) phase of the pressure which elicit channel opening, at 3 and 10 Hz not each positive phase is efficient

The membrane potential is clamped at -186 mV. MSL10 protein is transiently expressed in quintuple msl4;msl5;msl6;msl9;msl10 mutant (Δ5) protoplasts. Ionic conditions are described in the Materials and Methods

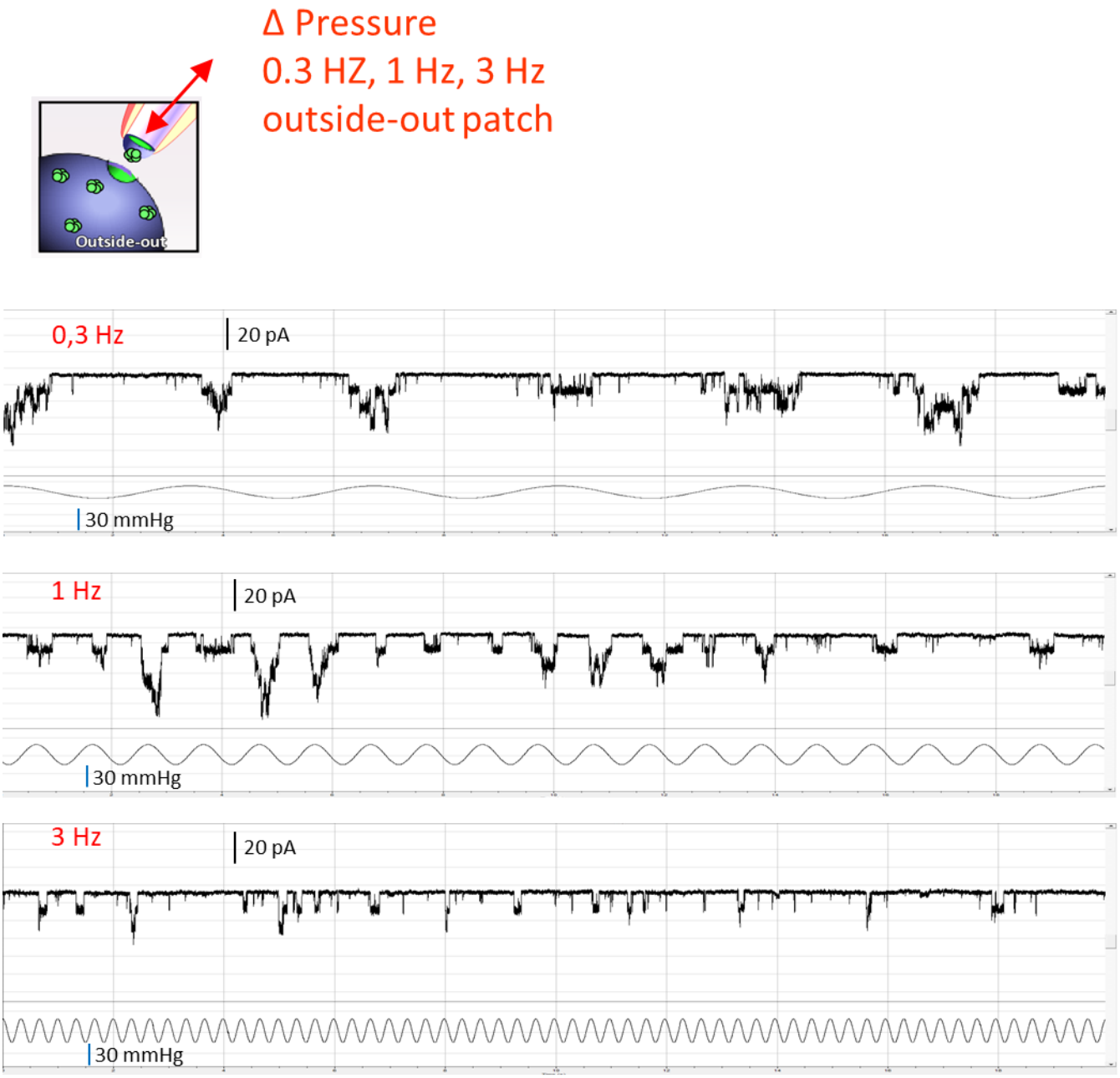

Fig. S4. Patch clamp recording of MSL10 elicited by oscillatory pressure of 0.3 Hz, 1 Hz, 3 Hz.

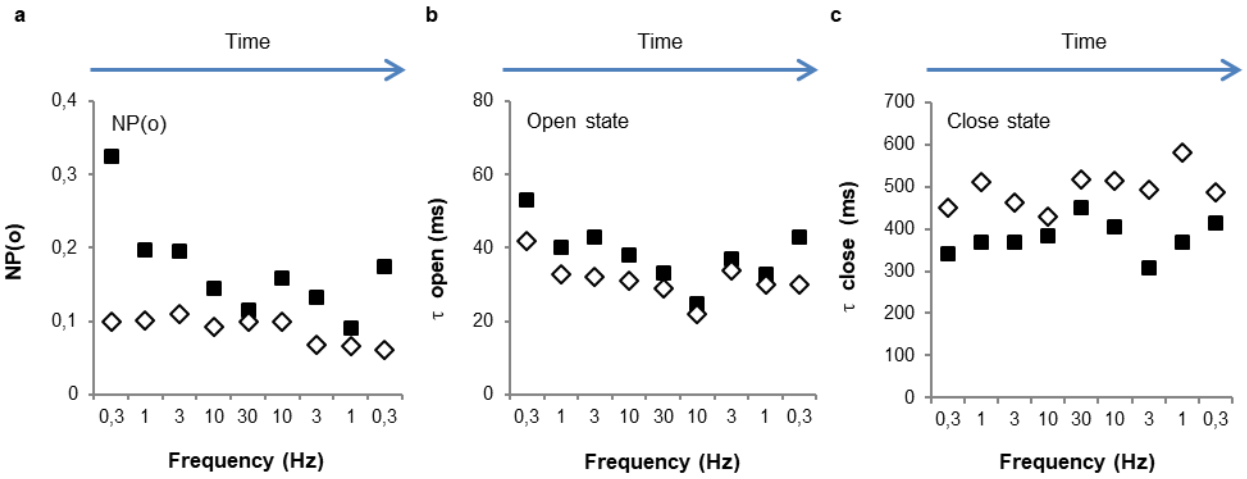

Fig. S5. MSL10 channel characteristics obtained on an individual patch using a protocol alternating oscillatory and static stimulation. The same protocol as Figure 3a alternating oscillatory and static stimulation was applied to excised outside-out-patches a-c, Representative single patch analysis at different frequencies (*black square*) compared to static stimulation (*white square*). Effects of frequency stimulation on a, open probability NP(o), b, open state time constant τ_{open} and c, closed state time constant τ_{close} .

The membrane potential is clamped at -186 mV. MSL10 protein is transiently expressed in quintuple *msl4;msl5;msl6;msl9;msl10* mutant (*Δ5*) protoplasts. Ionic conditions are described in the Materials and Methods.